Indian Journal of Chemistry
Vol. 65, July 2026, pp. 663-679
DOI: 10.56042/ijc.v65i7.31218

Methylene resonance and conjugation effects in 3-(4-bromophenyl)-5-(substituted phenyl)-4,5-dihydroisoxazoles: Synthesis, spectral QSAR studies, *in silico* and *in vitro* activities evaluation

P Sudha[a], S Balasundari[a], K Devika[b], I Muthuvel[a,c] & G Thirunarayanan*[a]

[a] Department of Chemistry, Annamalai University, Annamalainagar 608 002, Tamil Nadu, India

[b] Department of Chemistry, Thiru. Vi. Ka. Government Arts College, Thiruvarur 610 003, Tamil Nadu, India
(Affiliated to Bharathidasan University, Tiruchiarppalli 620 024, Tamil Nadu, India)

[c] Department of Chemistry, M. R. Government Arts College, Mannargudi 614 001, Tamil Nadu, India
(Affiliated to Bharathidasan University, Tiruchirappalli 620 024, Tamil Nadu, India)

E-mail: drgtnarayanan@gmail.com, thirunarayanan.g.10313@annamalaiuniversity.ac.in

Received 13 May 2026; accepted (revised) 20 July 2026

In this study we report the synthesis and biological evaluation of series of 3-(4-bromophenyl)-5-substituted phenyl-4,5-dihydroisoxazoles (**1-8**). These 3-(4-bromophenyl)-5-substituted phenyl-4,5-dihydroisoxazoles have been successfully synthesised from 4-bromophenyl chalcone derivatives with hydroxylamine hydrochloride by condensation cum cyclisation method, and their structures are confirmed by FT-IR, ^{1}H, and ^{13}C NMR spectroscopy techniques. The characteristic spectral frequencies and chemical shifts of these isoxazolines have been correlated with Hammett substituent constants and F, R parameters by QSAR analysis. The antimicrobial activity of synthesised isoxazolines (**1-8**) have been assessed *in vitro* against two Gram-positive and two Gram-negative bacterial strains, *Staphylococcus aureus*, *Enterococcus faecalis*, *Escherichia coli*, and *Klebsiella pneumonia* and two fungal strains *Candida aureus*, *Candida albicans* by Kirby-Bauer disc diffusion method. The molecular structure of 3-(4-bromophenyl)-5-substituted phenyl-4,5-dihydroisoxazoles has been explored using Density Functional Theory (DFT) at the B3LYP/6-311G(d,p) level of theory. The simulations yield information about total energy, frontier molecular orbitals (HOMO and LUMO), and molecular electrostatic potential (MEP) surfaces. Molecular docking investigation of 3-(4-bromophenyl)-5-substituted phenyl-4,5-dihydroisoxazoles (**1–8**) against the bacterial protein DNA gyrace (PDB ID: 4URO) reveals that compound **8** has the highest binding affinity value (–6.68 kcal/mol). The findings of the ADMET (Absorption, Distribution, Metabolism, Excretion, and Toxicity) study help the ongoing development of pharmacologically active medicines.

Keywords: QSAR analysis, DFT, Isoxazolines, ADMET

Heterocyclic compounds are increasing significance due to their ability to act as a bridge between chemical and biological research[1]. Heterocyclic chemistry is important in the design and development of new medicinal compounds since most medications contain heterocyclic rings[2]. In 2020, the US FDA authorized 24 small compounds, of which 22 had heterocyclic moieties. The study of heterocyclic compounds has received great attention due to its amazing pharmacological potential, promoting extensive research in recent years. Among these molecules, nitrogen and oxygen containing heterocycles have proven extremely beneficial, making them an excellent choice for further study[3]. The chemistry of chalcones has inspired scientists to explore innovative synthetic methods because they have a natural group in their structure, which provides a major benefit to understanding the pharmacology of substances such as antiviral, antifungal, anticancer, and antioxidant. In this study, chalcone derivatives were produced by condensation of aromatic ketone with substituted aromatic aldehydes in an alkaline medium[4]. Chalcones can be readily synthesized by chemically utilizing a variety of reaction techniques and approaches. One popular technique to create the title compound through carbonyl derivative by Claisen-Schmidt condensation method, this is one of the famous methods for synthesising chalcone[5]. To the best of our knowledge, chalcones are an important precursor for the development of a new chalcone chemical featuring the isoxazoline moiety[6]. The isoxazoline ring is an essential heterocyclic moiety which comprises one nitrogen atom next to one oxygen atom in a five-membered ring structure along

with a double bond[7]. In recent years, the isoxazoline moiety has piqued the interest of people working in the drug industry, because it can be found among numerous naturally occurring molecules that were effective in medicine and agriculture. In relatively simple to manufacture and chemical manipulation involve both bonding of isoxazoline with substituted aromatic and non-substituted aromatic, which are usually low toxicity[8]. The reactive intermediate chalcones involved in their synthesis also exhibit wide range of biological activities[9]. The isoxazole ring has enhanced pharmacological activity because its two neighbouring electronegative heteroatoms provide hydrogen donor-acceptor interactions with a number of target enzymes and receptors that other ring systems are unable to access. The synthesis of functional isoxazoles is evidently of great interest, as indicated by the fact that the isoxazole ring is the 33rd most common of the 351 ring systems found in currently marketed drugs[5]. Many pharmaceutical substances, especially, the anticonvulsant zonisamide[10,11], nonsteroidal anti-inflammatory drug Valdecoxib[12] and the antirheumatic Leflunomide contain the isoxazole scaffold. Similarly, chemicals produced from isoxazoles, such as sulfamethoxazole[13], sulfisoxazole[14], and oxacillin[15] are only used professionally to treat bacterial infections. Cloxacillin[16], Dicloxacillin, and Flucloxacillin[17] are examples of β-lactamase-resistant antibiotics with isoxazole pharmacophore. Cyclorine[18] is a naturally occurring antibiotic with an isoxazole moiety that has antitubercular effects. Many isoxazole compounds exhibit anti-HIV and anticancer properties, such as, Acivicin[5] and maytansine[19]. Antimicrobial investigations combined with quantitative structure activity relationships (QSAR) studies for drug development are extremely significant technologies in the medical and pharmaceutical fields[20]. Molecular docking studies are particularly essential in drug design because they can predict the likely interactions between possible therapeutic molecules (ligands) and their target proteins (enzymes or receptors)[21]. Based on literature report, as stated by our knowledge, there is no information availed for 4-bromophenyl moiety isoxazoline compounds. Hence, the authors fascinated for the synthesis, characterization, spectral QSAR, molecular docking, DFT, ADMET *in-silico* and *in-vitro* activities of entitled compounds.

Result and Discussion

Spectral correlation studies

IR spectral correlation of isoxazolines

The infrared C=N stretching frequencies (ν, cm^{-1}) of synthesised isoxazolines have been align with Swain-Lupton's parameters[22] and Hammett substituent constants[23]. These results are presented in Table S1 (See Table S1, Supplementary Information for statistical analysis results). The infrared stretching frequency (ν, cm^{-1}) of C=N shows satisfactory correlation with F parameter, it shows positive ρ value. $\nu_{C=N}$ stretching frequency of synthesised isoxazoline derivatives shows poor correlation with Hammet substituent constant (σ, σ^+, σ_I, σ_R) and Swain Lupton parameter R. These constants incorporate with negative ρ values. This study found that the reverse substituent effect preserves the $\nu_{C=N}$ stretching frequency values in all substituted 5-(4-bromophenyl)-3-phenyldihydroisoxazole compounds. Lack of correlation with those parameters arises from the negligible influence of polar, field, and inductive factors, rendering them ineffective in predicting variations in νC=N bands[20]. This observation aligns with the methylene resonance and conjugative structure depicted in Fig. 1(a and b). The effect of substituent also influences the correlation factors.

Single regression analyses have revealed weak connections between F and R parameters and Hammett substituent constants. As a result, multi-regression analysis was chosen. The regression equations are assembled in Table S2 (see Table S2, Supplementary Information for multi-regression analysis results and its equations) provide satisfactory correlations νC=N stretching frequency with

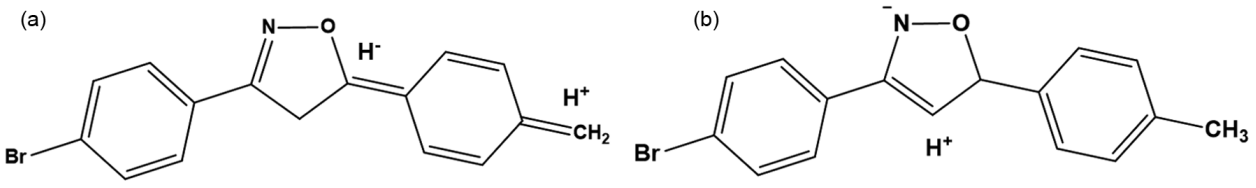

Fig. 1 — Methylene and Conjugative resonance structure of 3-(4-bromophenyl)-4,5-dihydro-5-*p*-tolylisoxazole

Hammett substituent constants and Swain – Lupton's parameters[22].

^{1}H NMR spectral correlations

The protons in isoxazolines existed and identified as AB or AA′ systems, respectively. In this series of isoxazolines, H_a proton chemical shifts (ppm) occur at greater fields than those of H_b and H_c. This is due to the deshielding of H_b and H_c, which have different chemical and magnetic environments[22-27]. The isoxazoline ring's assigned H_a, H_b, and H_c proton chemical shifts (ppm) have been associated with a number of Hammett substituent constants and Swain-Lupton's parameters. These results are presented in Table S1 (see Table S1, Supplementary Information for statistical analysis results). The ^{1}H NMR results for Ha proton of isoxazoline derivatives with Hammett coefficients σ (0.919) and σ^+ showed excellent correlations. Except for the parent and *p*-methyl, all other synthesized isoxazoline derivatives have an acceptable correlation with the Hammett constants σ_I and F.

Except *o*-fluoro all other isoxazolines shows good correlation with Hammett constant σ_R, satisfactory correlation with F parameter of Ha proton chemical shift (ppm) of all synthesised isoxazoline derivatives except *o*, *p*-fluoro isoxazoline. All correlations produce positive ρ values. This demonstrates that the usual substituent effect occurs in all systems. The conjugative structure depicted in Fig. 1 is responsible for the correlation failure. The H_b proton chemical shifts (ppm) with Hammett substituent constants and F and R parameters do not correlate. Positive ρ values are obtained from all correlations. This demonstrates that all systems exhibit the typical substituent effect. The methylene resonance and conjugative structure depicted in Fig. 1 is linked to the correlation failure. Table S1 (see Table S1, Supplementary Information for statistical analysis results) displays the findings of a statistical investigation of H_c proton chemical shifts (ppm) with Hammett substituents. There is no link between the H_c proton chemical shifts with Hammett substituent constants and the F and R parameters. All correlations generate negative ρ values. This study found that all substituted 5(4-bromophenyl)-3-phenyl dihydroisoxazole compounds exhibit the reverse substituent effect in terms of H_c proton NMR chemical shifts (δ, ppm). To confirm the ^{1}H NMR chemical shifts (δ, ppm) values with different Hammett substituent constants, F, and R parameters, a multi-parameter correlation analysis was performed after certain single parameter correlations failed. In multiple regression analysis satisfactory correlation was obtained. The correlation equations for Ha–Hc protons are given in Table S2 (see Table S2, Supplementary Information for multi-regression analysis results and its equations).

^{13}C NMR spectral correlations

The ^{13}C NMR chemical shifts (δ, ppm) of C=N, C-X, and CH_2 carbons of 4-bromophenyl isoxazoline derivatives are connected with Hammett σ, σ^+, σ_I, σ_R constants, F, and R parameters. Table S1 (See Table S1, Supplementary Information for statistical analysis results) shows statistical results for δC=N chemical shifts (ppm) with Hammett substituents. The δC=N chemical shifts with Hammett substituent constants and F and R parameters do not correlate. Correlations with σ, σ_R and R produce positive ρ values, hence these correlations show normal substituent effect. Other Hammett substituent constant and F parameters produce negative ρ values. This indicates that those correlations have reversible substituent effect operate in all system. The failure in correlation is associated with the conjugative structure shown in Fig. 1. ^{13}C NMR data for isoxazoline ring CH_2 of the isoxazoline derivatives (1-8) with Hammett constants σ (r=0.919) and σ^+ has shown satisfactory correlations, Swain-Lupton parameter F shows poor correlation
(r = 0.853) and produce satisfactory correlation with σ_R, σ_I, and R parameter except H, 4-CH_3, 2-F, 4-F. All correlation produces negative ρ values. This indicates that those correlations have reversible substituent effect operate in all system. ^{13}C NMR data for C-X of the isoxazoline derivatives with Hammett constants (r > 0.9) has shown satisfactory correlations with positive ρ values for Hammett constants σ, σ^+, σ_I, and F parameters. This shows normal substituent effect operates in all system. The negative ρ values obtained for Hammett constant σ_R, and F parameter. This result shows reversible substituent effect operate throughout the system. The authors believe it is worthwhile to look for multiple linear regression analysis since some of the Hammett constants are unable to establish individually sufficient correlation and the corresponding equations are provided in Table S2 (see Table S2, Supplementary Information for multi-regression analysis results and its equations).

Density functional theory (DFT) analysis

Frontier molecular orbital analysis

To acquire some information about the structures of the compounds, a molecular modelling studies was

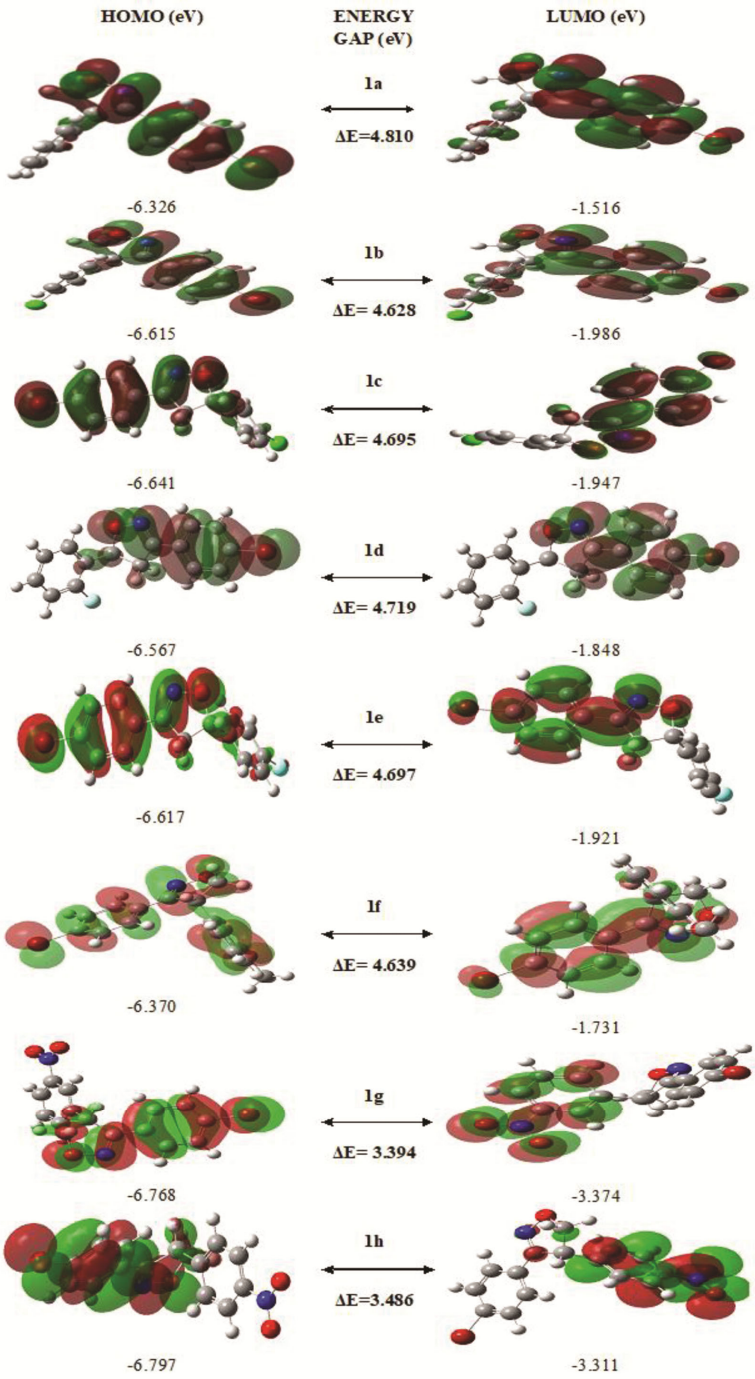

Fig. 2 — Frontier molecular orbitals of synthesised isoxazolines

conducted utilizing the Gaussian 09 W tool through B3LYP/6-311G (d,p). Quantum chemical calculations, involving the frontier molecular orbitals (HOMO LUMO), can predict the molecular structure, chemical features, and chemical behaviour of compounds. These calculations describe how the molecule interacts with other molecules[28].

The frontier molecular orbital refers to the molecular orbitals where HOMO acts as an electron donor and LUMO work as an electron acceptor[29]. The HOMO, LUMO pictures, energy values and energy gap values of synthesised Isoxazolines are listed in Fig. 2. The green and red colour region of frontier molecular orbitals signifies positive and negative

wave functions are generated. The HOMO energies are ranging from -6.326 to -6.797 eV. The LUMO energies are ranging from -1.516 to -3.374 eV. The energy gap values of synthesised isoxazolines (1-8) are ranged between 3.394 and 4.810 eV. The energy needed for electronic transitions, which are essential for molecular reactivity, is indicated by the energy gap (ΔE) value. From the frontier molecular orbitals result shows compound **7** have lowest energy gap value compared with other synthesised compounds. Hence compound **7** have highest reactivity but less stable and compound **1** have highest energy gap value, it shows less reactivity and high stability. The energy gap values for synthesized isoxazolines are arranged in ascending order: 7<8 < 2 < 6 < 3 < 5 < 4 < 1. These results reveal that substituent and position of the substituent also enhance the reactivity of the synthesised isoxazolines.

Global reactivity analysis of 3-(4-bromophenyl)-5-substituted phenyl-4,5-dihydroisoxazoles

The FMO method was used to calculate reactivity data, such as electron affinity (EA), ionization energy (IP), electronegativity (χ), softness (σ), and hardness (η). EHOMO is related to ionisation energy. Which provides information on how an electron is removed from a molecule[30]. These values are tabulated in Table 1.

The ionization energy of synthesised isoxazoline are ranging from 6.326 to 6.797 eV. Electron affinity (EA) has a significant impact on chemical reactivity. The EA is the amount of energy released when an electron is added to a molecule. The electron affinity values are ranging from 1.516 to 3.374 eV. Moreover, compound **7** has the highest electron affinity value, it has the strongest tendency to gain an electron and create a negative ion. This suggests that **7** is the most accepting of electrons. On the other hand, compound **1** has least value and it has least reactivity. A molecule's softness and hardness can also be used for evaluating its polarizability. More polarizable molecules have lower hardness values and higher softness values. Compound **7** has higher softness value and lower hardness value, hence compound **7** has a more polarizability and reactivity. Compound **1** has lowest softness value and highest hardness value hence it least polarizability and reactivity, but more stable. Electronegativity (χ) refers to a molecule's ability to attract electrons from other molecules when they interact. Higher electronegativity levels indicate a stronger ability to attract electrons[31]. The synthesized compounds have electronegativity values between 3.921 and 5.071 eV. The highest electronegative value is found in compound **7**. The electronic chemical potential (μ), which ranges from -5.071 to -3.921 eV, helps forecast how a molecule will interact with other chemical species and provides insight into the distribution of charges within the molecule. A molecule's capacity to take electrons during a chemical reaction is measured by electrophilicity indices, which range from 3.197 to 7.576 eV. It measures how likely a molecule is to behave as an electrophile.

Molecular electrostatic potential (MEP) surfaces

The MEP is an excellent tool for visualizing areas of a molecule that are susceptible to electrophilic or nucleophilic assault. In most MEPs, the red region (negative) represents areas of high electron density, which are appealing to electrophiles, while the blue region (positive) represents areas of low electron density, which are attracted to nucleophiles. The MEP helps to understand a molecule's reactivity, polarity, and intermolecular interactions by demonstrating its size, shape, and electrostatic potential distribution[31]. Fig. 3 illustrates the MEP of the investigated

Table 1 — Computed global metrics for synthesised 3-(4-bromophenyl)-5-substituted phenyl-4,5-dihydroisoxazoles

Compd	IP eV	EA eV	(ΔE) eV	(η) eV	(σ) eV^{-1}	(μ) eV	(χ) eV	(ω) eV
1	6.326	1.516	4.810	2.405	0.208	–3.921	3.921	3. 197
2	6.615	1.986	4.628	2.314	0.216	–4.301	4. 301	3. 996
3	6.641	1.947	4 .695	2. 347	0.213	–4.294	4. 294	3. 928
4	6.567	1. 848	4. 719	2. 360	0.212	–4.208	4. 208	3. 752
5	6.617	1.921	4. 697	2. 348	0.213	–4.269	4. 269	3. 880
6	6.419	1.774	4. 645	2. 323	0.215	–4.096	4. 096	3. 612
7	6. 768	3.374	3.394	1.697	0.295	–5.071	5.071	7.576
8	6. 797	3.311	3.486	1.743	0.287	–5.054	5.054	7.327

IP- ionization potential, EA- electron affinity, ΔE- energy gap, η - hardness, σ- softness, μ - chemical potentials, χ - electronegativity, ω – electrophilicity.

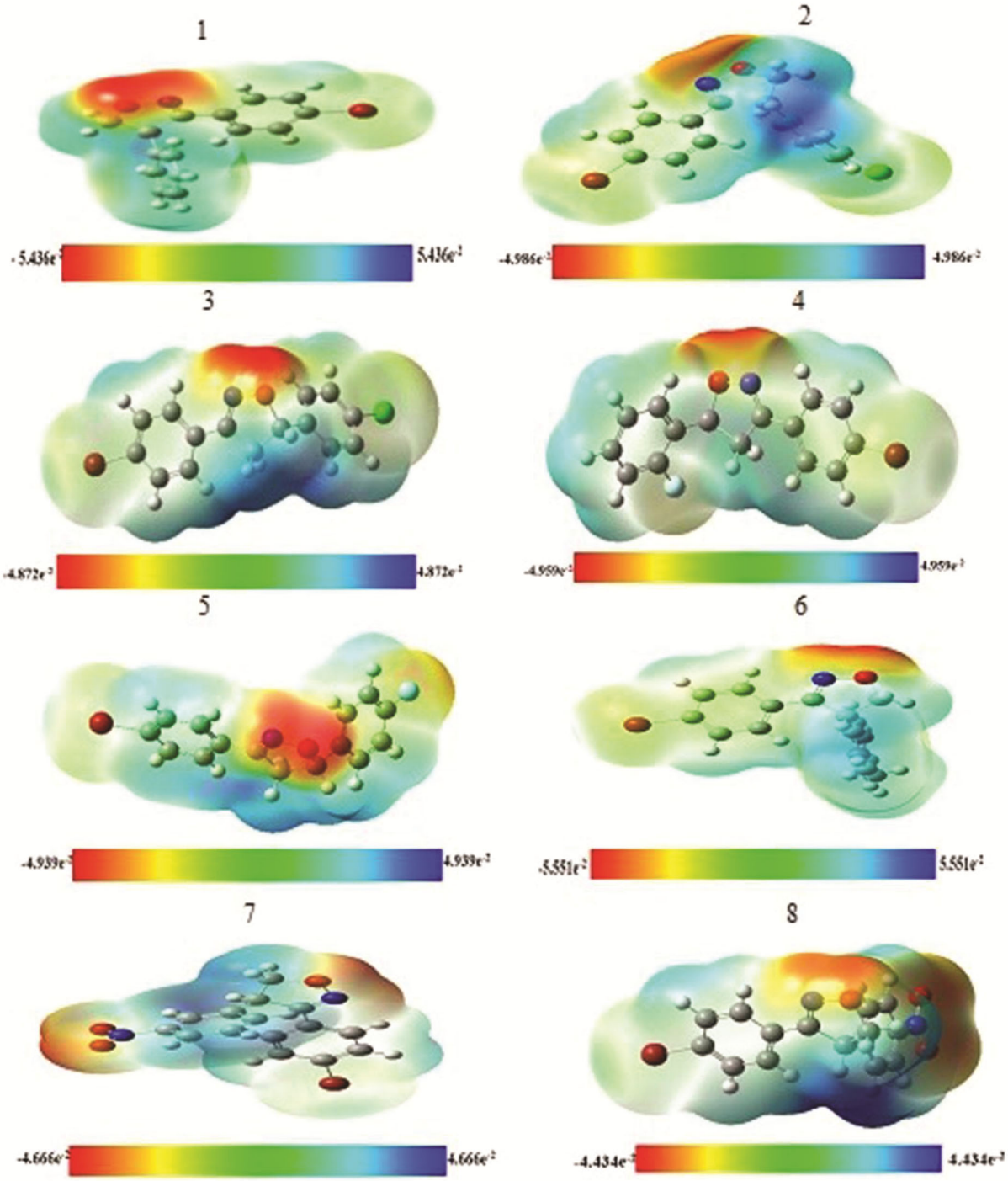

Fig. 3 — Molecular electrostatic potential of 3-(4-bromophenyl)-5-substituted phenyl-4,5-dihydroisoxazoles

compounds. The most negative region is located around the oxygen connected to the isoxazoline ring, indicating that it is a good target for electrophilic assaults. Positive potentials are typically seen around the hydrogens of the isoxazoline ring, indicating that this location is susceptible to nucleophilic attacks.

Molecular docking analysis of 3-(4-bromophenyl)-5-substituted phenyl-4,5-dihydroisoxazoles

The molecular docking study of the synthesized 4-bromophenyl isoxazolines were studied using the protein binding ability to DNA gyrase enzyme (PDB ID: 4URO) bacterial protein[32]. The results of

molecular docking study of 3-(4-bromophenyl)-5-substituted phenyl-4,5-dihydroisoxazoles are listed in the Table 2. From these results all the compounds show almost similar binding energy values is ranging from -6.07 to -6.62 kcal/mol. Compound 8 has highest binding affinity (-6.62 kcal/mol) with targeted protein 4URO. It has two conventional hydrogen bond interaction with LEU.C:25 and ALA.C:28, hydrophobic interactions of alkyl, pi-alkyl interaction with VAL.C:107, ILE.C:102, VAL.C:105, VAL.C:130. Compound **5** shows lowest binding affinity with targeted protein; As a result, its activity level is moderate. The docking results show that all produced compounds have good antibacterial action except compound **5,** because these compounds (**1-4** and **6-8**) have a good binding affinity with the 4URO protein.

ADMET (Absorption, Distribution, Metabolism, Excretion and Toxicity) analysis

The graphical representation for the drug-like properties of synthesized 3-(4-bromophenyl)-5-

Table 2 — Molecular docking analysis of 3-(4-bromophenyl)-5-substituted phenyl-4,5-dihydroisoxazoles

Entry	2D Pose	3D Pose	H-bond interaction	Other interactions	Interaction types	Binding energy (kcal/mol)
1	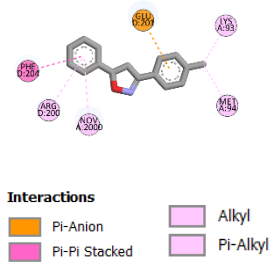	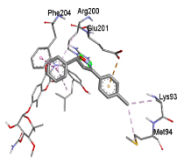		GLU.D:201 PHE.D:204 LYS.A:93 MET.A:94 ARG.D:200	Pi-anion Pi-Pi stacked Alkyl Alkyl Pi-Alkyl	–6.16
2	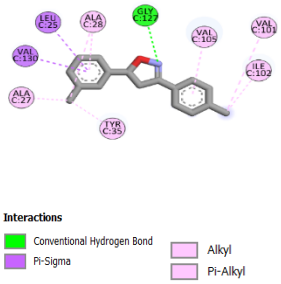	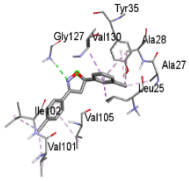	GLY.C: 127	LEU.C:25 VAL.C:130 VAL.C:105 VAL.C:101 ILE.C:102 TYR.C:35 ALA.C:27	Pi-Sigma Pi-Sigma Pi-Alkyl Pi-Alkyl Alkyl Alkyl Alkyl	–6.59
3	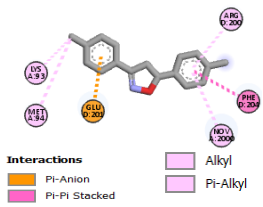	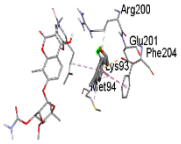		GLU.D:201 PHE.D:204 LYS.A:93 MET.A:94 ARG.D:200	Pi-anion Pi-Pi stacked Alkyl Alkyl Pi-Alkyl	–6.49
4	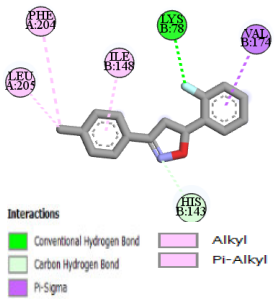	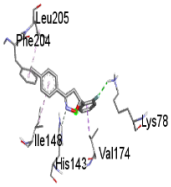	LYS.B:78 HIS.B:143	VAL.B:174 LEU.A:205 PHE.A:204 ILE.B:148	Pi-Sigma Alkyl Alkyl Pi-Alkyl	–6.23

(Contd.)

Table 2 — Molecular docking analysis of 3-(4-bromophenyl)-5-substituted phenyl-4,5-dihydroisoxazoles *(Contd.)*

2D Pose	3D Pose	H-bond interaction	Other interactions	Interaction types	Binding energy (kcal/mol)	
5	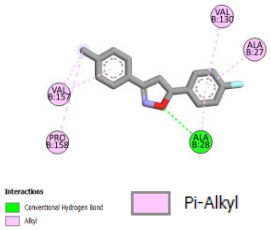	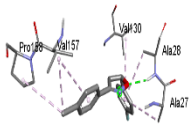	ALA.B:28	PRO.B:158 VAL.B:157 VAL.B:130 ALA.B:27	Alkyl Alkyl Pi-Alkyl Pi-Alkyl	–6.07
6	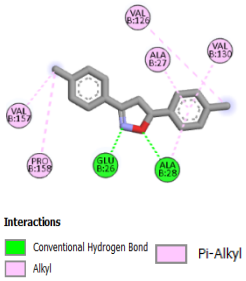	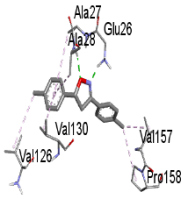	GLU.B:26 ALA.B:28	VAL.B:126 VAL.B:157 PRO.B:158 VAL.B:130 ALA.B:27	Alkyl Alkyl Alkyl Pi-Alkyl Pi-Alkyl	–6.48
7	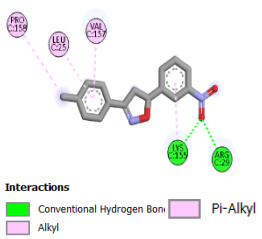	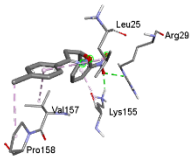	LYS.C:155 ARG.C:29	PRO.C:158 LEU.C:25 VAL.C:127	Alkyl Pi-Alkyl Pi-Alkyl	–6.47
8	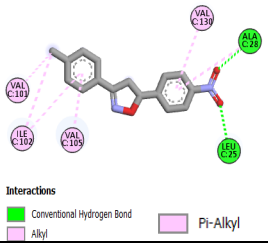	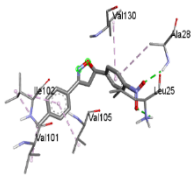	LEU.C:25 ALA.C:28	VAL.C:107 ILE.C:102 VAL.C:105 VAL.C:130	Alkyl Alkyl Pi-Alkyl Pi-Alkyl	-6.62

substituted phenyl-4,5-dihydroisoxazole derivatives were shown in Fig. 4. The synthesised compounds were evaluated for drug-likeness based on Lipinski's rule of five and their ADMET properties using online tools such as SwissADME and protox. To evaluate a potential drug candidate, it should meet Specific physicochemical criteria include a maximum of 5 hydrogen-bond donors (HBDs).

Ten hydrogen-bond acceptors (HBAs), a molecular weight of less than 500 Da, a log P value of no more than 5, and a total polar surface area (TPSA) of no more than 140 Å (Ref. 33). The physicochemical properties of synthesised compounds are shown in the Table 3. According to the SwissADME data, all synthesized molecule complies with Lipinski's rule of five. The physicochemical properties predictions of compounds imply that all compounds possess the drug like properties. The results conceded that no violation is found in agreement with Lipinski's rule of five. Additionally, the compounds' molecular masses

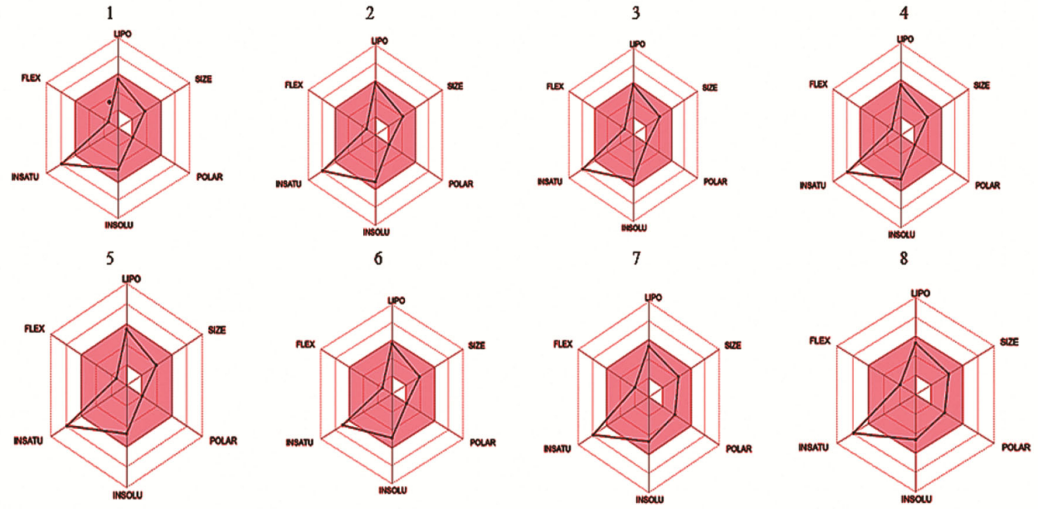

Fig. 4 — ADME radar structure of 3-(4-bromophenyl)-5-substituted phenyl-4,5-dihydroisoxazoles

Table 3 — Physicochemical properties of 3-(4-bromophenyl)-5-substituted phenyl-4,5-dihydroisoxazoles

Compd	Lipinski's Violations (≤1)	Based on Lipinski 's Rule				Veber's rule		
		MW (≤500)	HBA (≤10)	HBD (≤5)	MLOGP	NROTB (≤10)	TPSA (130Å)	ABS%
1	0	302.17	2	0	3.65	2	21.59	101.55
2	1	336.61	2	0	4.16	2	21.59	101.55
3	1	336.61	2	0	4.16	2	21.59	101.55
4	1	336.61	2	0	4.16	2	21.59	101.55
5	0	320.16	3	0	4.04	2	21.59	101.55
6	0	316.19	2	0	3.89	2	21.59	101.55
7	0	347.16	4	0	3.38	3	67.41	85.75
8	0	347.16	4	0	3.38	3	67.41	85.75

ranged from 302 to 347 a.m.u. While the hydrogen bond acceptor values range from two to four, the number of hydrogen bond donor atoms is zero. All compounds have total polar surface area (TPSA) values between 21.59 and 67.41 (below 140 Å). Since they can more readily pass through biological membranes, it is widely acknowledged that substances with a TPSA value of 140 Å or less are more likely to be well absorbed. Isoxazolines may have favourable absorption properties because their TPSA values are all below the 140 Å threshold. These findings indicate that the compounds can be efficiently absorbed *via* the gastrointestinal tract (GIT) and penetrate the blood brain barrier. Furthermore, a bioavailability score of 0.55 suggests biological activity. Compounds with a score above 0 are more likely to be absorbed and circulate throughout the body, which is essential for therapeutic effects. These substances demonstrated a high potential for absorption in the human gastrointestinal tract (GIT), according to the ADMET property study.

This is a useful discovery because effective absorption is necessary for a medication to reach systemic circulation and have its therapeutic effect[34]. Enzymes like CYP1A2 inhibitor (for A1), CYP2C19 inhibitor, CYP2C9 inhibitor (for all medications), CYP2D6 non-inhibitor, and CYP3A4 non-inhibitor metabolize it. Pharmacokinetic properties of 3-(4-bromophenyl)-5-substituted phenyl-4,5-dihydro-isoxazoles are summarized in Table 4. These enzymes aid in the process of oxidation and elimination. It is not inherently carcinogenic and has no harmful value[35].

Toxicity prediction

Accurate toxicity prediction is essential for minimizing expenses and efforts in preclinical and clinical trials[36]. To assess the toxicity profiles of 3-(4-bromophenyl)-5-substituted phenyl-4,5-dihydroisoxazoles, researchers used web-based tools such as Protox II, with results presented in Table 5.

For every medication, they calculated the median lethal dose (LD_{50}), which varied between 750 and 1000 mg/kg. The chemicals are categorized as being in toxicity class IV based on these values. The LD_{50} value indicates the amount of a drug that, when

Table 4 — Pharmacokinetic properties of 3-(4-bromophenyl)-5-substituted phenyl-4,5-dihydroisoxazoles

Compd	GI	BBB	P-gp	CYP1A2	CYP2C19	CYP2C9	CYP2D6	CYP3A4	Bio Availability score
1	High								0.55
2	High								0.55
3	High								0.55
4	High								0.55
5	High								0.55
6	High								0.55
7	High								0.55
8	High								0.55

Green Ellipse: Yes; **Red** Ellipse: No

provided all at once, would be predicted to cause death in fifty percent of the test animals[34]. Compounds with higher LD_{50} values are generally less harmful than those with lower LD_{50} values. Toxicity class design provides an organized way to express a compound's acute toxicity level[37]. Whereas class IV indicates moderate toxicity. These results suggest that compounds (1-8) show moderate toxicity. Alongside the acute toxicity assessment using LD_{50} values, an extensive assessment of the substances was conducted for other toxicity parameters such as hepatotoxicity, cytotoxicity, mutagenicity, carcinogenicity. These results revealed that all synthesised compounds have moderate toxicity. This information can assist researchers in predicting future toxicity issues and optimizing preclinical and clinical development techniques for these drugs.

Antimicrobial activity of 3-(4-bromophenyl)-5-substituted phenyl-4,5-dihydroisoxazoles

Antibacterial activity

The isoxazolines were screened for their antibacterial activity against two Gram-positive and two Gram-negative bacterial strains, *Staphylococcus aureus*, *Enterococcus faecalis*, *Escherichia coli*, and *Klebsiella pneumonia* by Kirby-Bauer disc diffusion method[38] chloramphenicol used as a reference drug. Table 6 shows the observed antibacterial activities and the Minimum Inhibitory Concentrations (MIC) values are given in parenthesis[39-48]. Zone of inhibition of synthesised compounds with reference drug petri dish were shown in Fig. 5. The graphical representation for antibacterial activity of synthesised compounds with reference drug are shown in Fig. 6. The investigation of antibacterial screening results indicates all compounds have an antibacterial activity against all

Table 5 — Toxicity prediction of 3-(4-bromophenyl)-5-substituted phenyl-4,5-dihydroisoxazoles

Compd	LD50 (mg/Kg)	Toxicity class	Organ toxicity			
			Hepatotoxicity	Cytotoxicity	Mutagenicity	Carcinogenicity
1	750	4				
2	820	4				
3	750	4				
4	750	4				
5	750	4				
6	750	4				
7	1000	4				
8	1000	4				

Green Ellipse: Yes; **Red** Ellipse: No

Table 6 — Antimicrobial activity of 3-(4-bromophenyl)-5-substituted phenyl-4,5- dihydroisoxazoles

Entry	Entry in dish	X	Zone of inhibition (mm)					
			Antibacterial				Antifungal	
			Gram positive		Gram negative			
			S. aureus	*E. faecalis*	*E. coli*	*K. pneumoniae*	*C. albicans*	*C. auris*
1	1c	H	8(15)	9(20)	14(15)	15(20)	10(15)	11(15)
2	1h	3-Cl	13(10)	12(20)	8(20)	11(15)	12(15)	10(15)
3	1a	4-Cl	8(20)	10(10)	5(10)	7(10)	10(15)	11(15)
4	1d	2-F	9(15)	7(15)	6(20)	7(10)	5(10)	7(10)
5	1e	4-F	17(15)	18(10)	13(15)	11(15)	13(15)	15(20)
6	1g	4-CH_3	8(15)	10(10)	11(10)	16(15)	9(10)	7(10)
7	1f	3-NO_2	6(20)	9(15)	12(20)	11(15)	5(10)	13(15)
8	1b	4-NO_2	20(20)	21(20)	19(15)	21(20)	17(20)	18(20)
	Reference		Chloramphenicol				Fluconazole	
			22(20)	23(20)	23(15)	23(20)	19(20)	21(20)

the examined pathogens. This is because of the presence of isoxazoline ring; hence it has two electron donor acceptor atoms nitrogen and oxygen atoms. It enhances the antibacterial activity. On the other hand, presence of substituent also produce effect on the antibacterial activity of synthesised compounds. Compound **8** shows an excellent activity against *Staphylococcus aureus*, *Enterococcus faecalis*, *Escherichia coli*, and *Klebsiella pneumonia.*

This is may be due to the presence of *p*-nitro group. Compound 2 and 5 shows good activity against *Staphylococcus aureus.* All other compounds show a moderate activity against *Staphylococcus aureus.* Compounds 2, 5,6 shows a good activity against

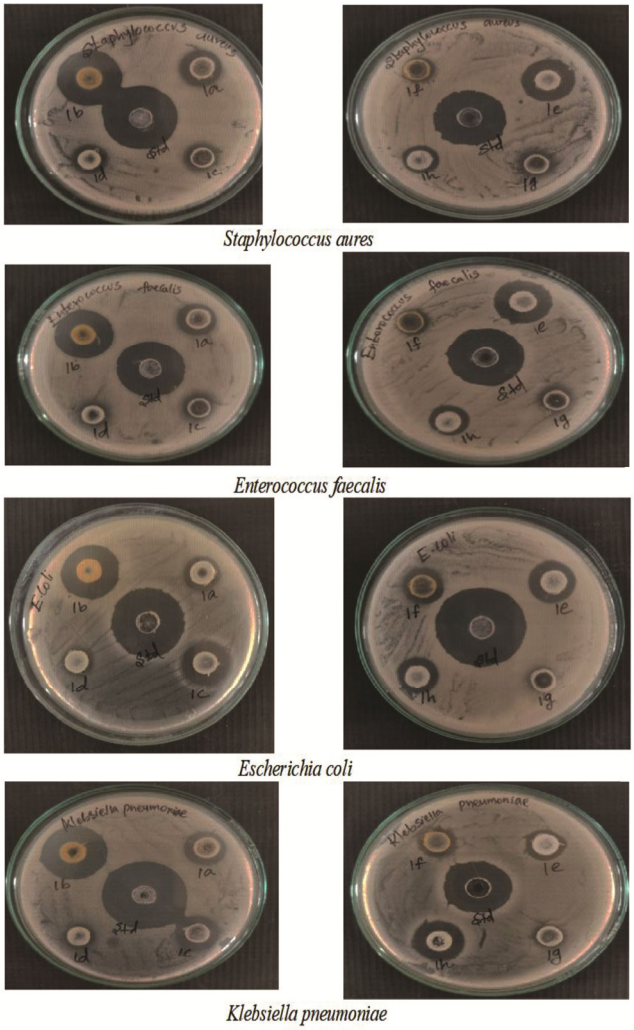

Fig. 5 — Antibacterial activity by means of petri-plates of 3-(4-bromophenyl)-5-substituted phenyl-4,5-dihydroisoxazoles

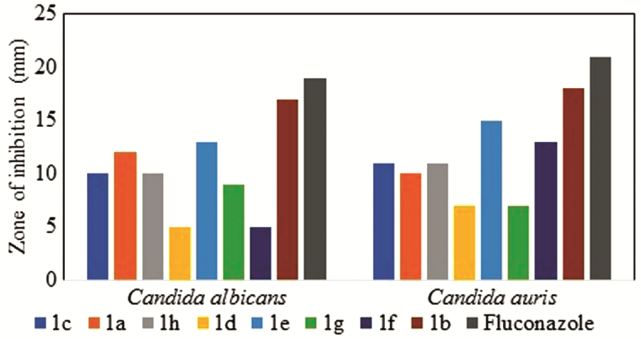

Fig. 6 — Graphical representation for antibacterial activity of synthesised isoxazolines

Enterococcus faecalis. Remaining compounds shows moderate activity against *Enterococcus faecalis.* Compounds 1, 5, 6, 7 and compounds 1, 2, 5, 6, 7 shows better activity against *Escherichia coli*, and *Klebsiella pneumonia.* This is because of the presence of + I, - I effect of the substituents such as 3-Cl, 4-F, 4-CH_3, 3-NO_2, 4-NO_2 and the resonance-conjugative structure shown in Fig. 1.

Antifungal activity

The synthesized isoxazolines were screened for their antifungal activity against two fungal strains *Candida aureus*, *Candida albicans* by Kirby-Bauer disc diffusion method[38] using chloramphenicol used as a reference drug. The observed antifungal activities in mm of zone of inhibition are presented in Table 6 and Minimum Inhibitory Concentrations (MIC) values for all the synthesized compounds are given in the parentheses[39-48]. Zone of inhibition of synthesised compounds with reference drug petri dishes are shown in Fig. 7. The graphical representation for antifungal activity of synthesised compounds with reference drug are shown in Fig. 8. The investigation of antifungal screening results indicates all compounds have an antifungal activity against all the examined pathogens. This is because of the presence of isoxazoline ring; hence it has two electron donor acceptor atoms nitrogen and oxygen atoms. It enhances the antifungal activity. On the other hand, presence of substituent also produce effect on the antifungal activity of synthesised compounds. Compound **8** shows an excellent activity against *Candida aureus*, *Candida albicans.* Except compounds **4, 6**, and **7** all other compounds (**1, 2, 3, 5**) produce good activity against *Candida aureus.* Compounds 1-3, 5, 6 shows a good activity against *Candida albicans*, compound 4, 6 produce low activity compared with other synthesised compounds. This is because of the presence of + I, - I effect of the substituents such as 3-Cl, 4-F, 4-CH_3, 3-NO_2, 4-NO_2 and the resonance-conjugative structure shown in Figure 1.

Experimental Section

Materials and methods

Reagent and solvents were purchased from TCI and Sigma – Aldrich chemicals. The melting points of synthesised isoxazoline were measured in open capillaries using Raga tech electrical melting point apparatus (uncorrected). Using an Agilent Cary-630N spectrophotometer, FT-IR spectra (KBr, 3000–800 cm^{-1}) were taken. The NMR spectra of ^{1}H (400 MHz) and ^{13}C (100 MHz) were obtained in $CDCl_3$ with TMS as an internal reference.

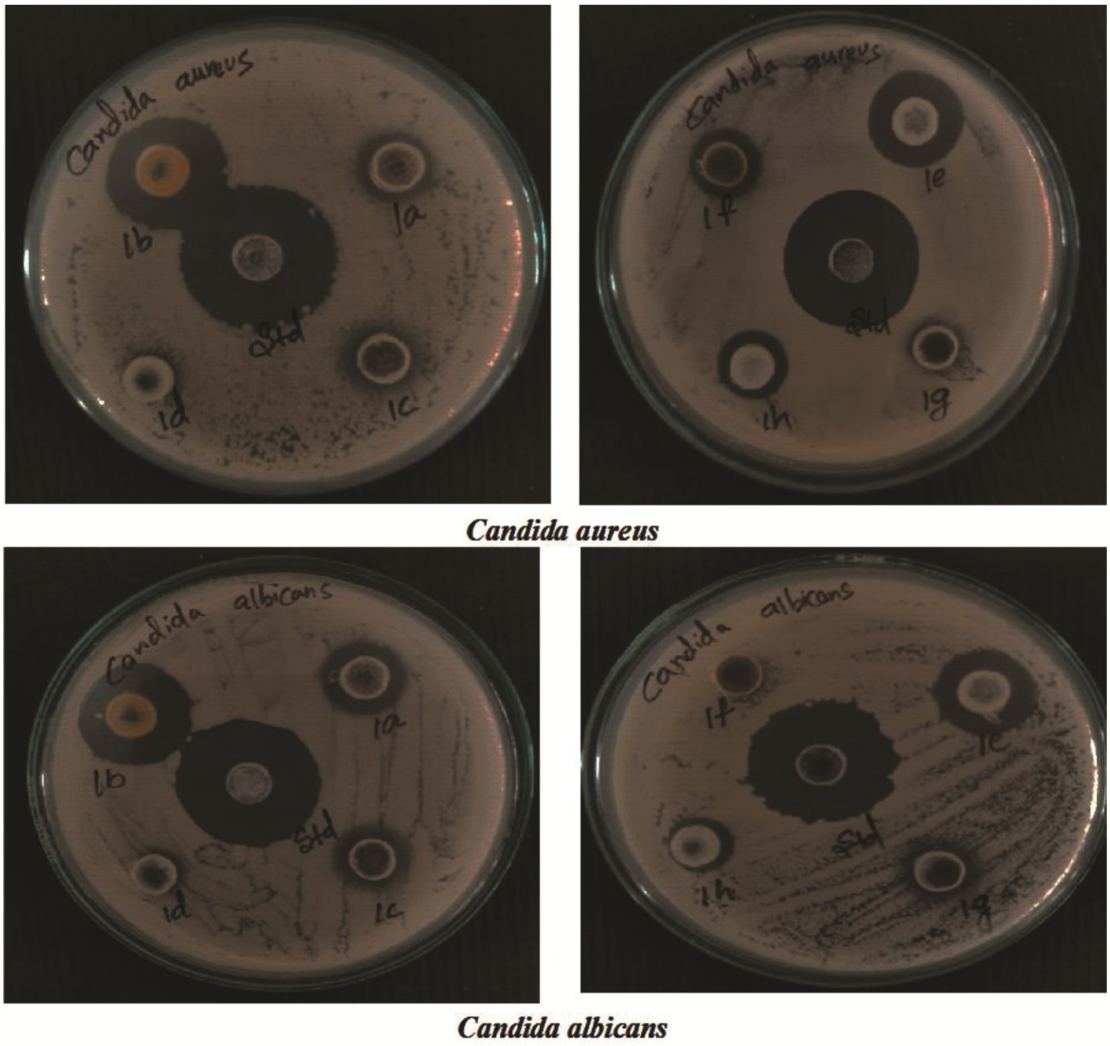

Fig. 7 — Antifungal activities (petri dishes) of 3-(4-bromophenyl)-5-substituted phenyl-4,5-dihydroisoxazoles

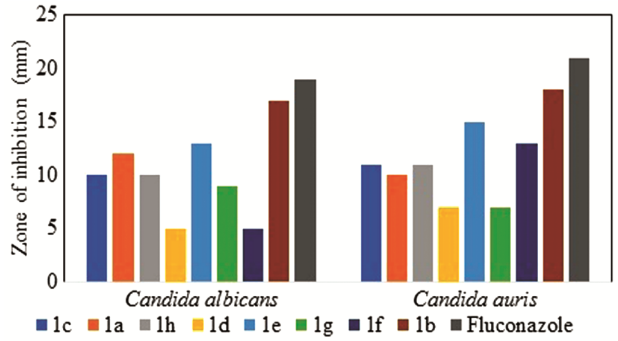

Fig. 8 — Chart representation for antifungal activity of 3-(4-bromophenyl)-5-substituted phenyl-4,5-dihydroisoxazoles

General procedure for the synthesis of 3-(4-bromophenyl)-5-substituted phenyl-4,5-dihydroisoxazoles

A combination of 4-bromo phenyl chalcones[49,50] (1 mmol), hydroxyl amine hydrochloride (1 mmol), and sodium hydroxide (2 mmol) was refluxed for 6-7 hours in 15 mL ethanol (Scheme 1). After the reaction was complete (as determined by TLC), it was cooled and placed into ice cold water. The curdy white precipitate was obtained, and the solid product was filtered, rinsed with cold water, dried, and recrystallized using ethyl alcohol. The physico-chemical parameters are summarized in Table 7.

Spectral data

The spectroscopic data of all synthesised isoxazolines are summarized here:

3-(4-Bromophenyl)-4,5-dihydro-5-phenylisoxazole, 1: IR (KBr): 3405 (aromatic C-H), 1618 C=N, 1074 C-O cm^{-1}; ^1H NMR (400 MHz, $CDCl_3$): δ 3.33 ($1H_a$, dd, $J_{(1,2)}$ =1.2Hz: $J_{(2,3)}$ = 1.6 Hz), 3.77 ($1H_b$, dd, $J_{(1,2)}$ =9.6Hz: $J_{(2,3)}$ = 4.4 Hz), 5.75 ($1H_c$, dd, $J_{(1,2)}$=0.8Hz:

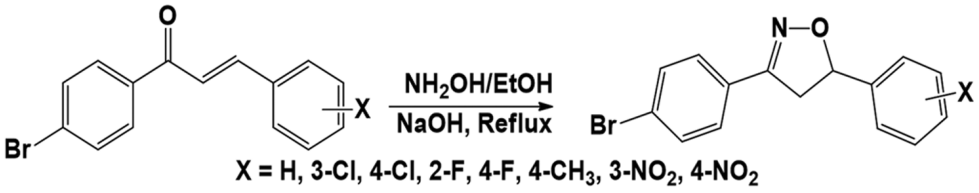

Scheme 1 — Synthesis of 3-(4-bromophenyl)-5-substituted phenyl-4,5-dihydroisoxazoles

Table 7 — Physical constant and analytical data of 3-(4-bromophenyl)-5-substituted phenyl-4,5-dihydro isoxazoles

Entry	X	Mol. Formula	Mol. Wt.	Time (h)	Yield (%)	m.p. (°C)
1	H	$C_{15}H_{12}BrNO$	302	6	90	105-106
2	3-Cl	$C_{15}H_{11}BrClNO$	336	7	92	108-109
3	4-Cl	$C_{15}H_{11}BrClNO$	336	7	94	111-112
4	2-F	$C_{15}H_{11}BrFNO$	320	6	89	88-89
5	4-F	$C_{15}H_{11}BrFNO$	320	6	90	92-93
6	4-CH_3	$C_{16}H_{14}BrNO$	316	8	90	143-144
7	3-NO_2	$C_{15}H_{11}BrN_2O_3$	347	7	88	141-142
8	4-NO_2	$C_{15}H_{11}BrN_2O_3$	347	7	92	140-141

$J_{(2,3)}$=0.8Hz), 6.0 (9H, m, Ar-H), 7.26-7.55; ^{13}C NMR (400 MHz, $CDCl_3$): δ 155.44 (C=N), 83.02 (C-O), 43.06 (CH_2), 124.56-140.79 (Ar-C).

3-(4-Bromophenyl)-5-(3-chlorophenyl)-4,5-dihydroisoxazole, 2: IR (KBr): 3146 (aromatic C-H), 1591(C=N), 1178 cm^{-1} (C-O); ^{1}H NMR (400 MHz, $CDCl_3$): δ 3.28 (1H$_a$, dd, $J_{(1,2)}$=8Hz: $J_{(2,3)}$ = 8 Hz)), 3.76 (1H$_b$, dd, $J_{(1,2)}$ =11.2Hz: $J_{(2,3)}$=10.8 Hz), 5.72 (1H$_c$, dd, $J_{(1,2)}$ =8Hz: $J_{(2,3)}$ = 8Hz), 7.26-7.54 (8H, m, Ar-H; ^{13}C NMR (400 MHz, $CDCl_3$): δ 155.39 (C=N), 82.08 (C-O), 43.15 (CH_2), 124.04-142.93 (Ar-C).

3-(4-Bromophenyl)-5-(4-chlorophenyl)-4,5-dihydroisoxazole, 3: IR (KBr): 3160 (aromatic C-H), 1616(C=N), 1223 cm^{-1} (C-O); ^{1}H NMR (400 MHz, $CDCl_3$): δ 3.36 (1H$_a$, dd, $J_{(1,2)}$ =8.4Hz: $J_{(2,3)}$ = 8Hz), 4.66 (1H$_b$, dd, $J_{(1,2)}$ =10.8Hz: $J_{(2,3)}$ = 11.2Hz), 5.53 (1H$_c$, dd, $J_{(1,2)}$ =8.4Hz: $J_{(2,3)}$ = 8Hz), 7.20-7.82 (8H, m, Ar-H); ^{13}C NMR ($CDCl_3$, 400 MHz): δ 155.29 (C=N), 82.10 (C-O), 42.99 (CH_2), 127.13-139.19 (Ar-C).

3-(4-Bromophenyl)-5-(2-fluorophenyl)-4,5-dihydroisoxazole, 4: IR (KBr): 3065 (aromatic C-H), 1595(C=N), 1157 cm^{-1} (C-O); ^{1}H NMR (400 MHz, $CDCl_3$): δ 3.27 (1H$_a$, dd, $J_{(1,2)}$ =6.4Hz: $J_{(2,3)}$ = 6.8Hz), 3.73 (1H$_b$, dd, $J_{(1,2)}$ =3.6Hz: $J_{(2,3)}$ = 2.8Hz), 5.72 (1H$_c$, dd, $J_{(1,2)}$ =12Hz: $J_{(2,3)}$ = 8Hz), 6.93-7.83 (8H, m, Ar-H); ^{13}C NMR (400 MHz, $CDCl_3$): δ 145.58 (C=N), 86.42 (C-O), 42.97 (CH_2), 124.55-137.80 (Ar-C).

3-(4-Bromophenyl)-5-(4-fluorophenyl)-4,5-dihydroisoxazole, 5: IR (KBr): 3065 (aromatic C-H), 1590(C=N), 1096 cm^{-1} (C-O); ^{1}H NMR (400 MHz, $CDCl_3$): δ 3.26 (1H$_a$, dd, $J_{(1,2)}$ =8Hz: $J_{(2,3)}$ = 8Hz), 3.75 (1H$_b$, dd, $J_{(1,2)}$ =12Hz: $J_{(2,3)}$ = 12Hz), 5.72 (1H$_c$, dd, $J_{(1,2)}$ =8Hz: $J_{(2,3)}$ = 8Hz), 6.79-7.80 (8H, m, Ar-H); ^{13}C NMR (400 MHz, $CDCl_3$): δ 156.81 (C=N), 82.25 (C-O), 42.95 (CH_2), 127.30-144.21 (Ar-C).

3-(4-Bromophenyl)-4,5-dihydro-5-p-tolylisoxazole, 6: IR (KBr): 2917 (aromatic C-H), 1646(C=N), 1113 cm^{-1} (C-O); ^{1}H NMR (400 MHz, $CDCl_3$): δ 3.29 (1H$_a$, dd, $J_{(1,2)}$ =8Hz: $J_{(2,3)}$ = 8.4Hz), 3.71 (1H$_b$, dd, $J_{(1,2)}$ =10.8Hz: $J_{(2,3)}$ = 11.2Hz), 5.71 (1H$_c$, dd, $J_{(1,2)}$ =8.8Hz: $J_{(2,3)}$ = 8.8Hz), 7.17-7.89 (8H, m, Ar-H), 2.35 (-CH_3); ^{13}C NMR (400 MHz, $CDCl_3$): δ 155.34 (C=N), 82.90 (C-O), 42.81 (CH_2), 120.47-145.55 (Ar-C) 21.28 (-CH_3).

3-(4-Bromophenyl)-4,5-dihydro-5-(3-nitrophenyl) isoxazole, 7: IR (KBr): 3084 (aromatic C-H), 1618(C=N), 1074 cm^{-1} (C-O); ^{1}H NMR (400 MHz, $CDCl_3$): δ 3.55 (1H$_a$, dd, , $J_{(1,2)}$ =8Hz: $J_{(2,3)}$ = 8Hz), 3.64 (1H$_b$, dd, $J_{(1,2)}$ =11.2Hz: $J_{(2,3)}$ =10.8Hz), 5.57 (1H$_c$, dd, $J_{(1,2)}$ =4Hz: $J_{(2,3)}$ =3.6Hz), 7.25-8.35 (8H, m, Ar-H); ^{13}C NMR (400 MHz, $CDCl_3$): δ 156.49 (C=N), 79.31 (C-O), 42.80 (CH_2), 123.52-133.84 (Ar-C).

3-(4-Bromophenyl)-4,5-dihydro-5-(4-nitrophenyl) isoxazole, 8: IR (KBr): 2917 (aromatic C-H), 1599(C=N), 1184 cm^{-1} (C-O); ^{1}H NMR (400 MHz, $CDCl_3$): δ 3.08 (1H$_a$, dd, $J_{(1,2)}$ =6Hz: $J_{(2,3)}$ =6Hz), 3.91

($1H_b$, dd, $J_{(1,2)}$ =4.4Hz: $J_{(2,3)}$ =10.4Hz), 4.43($1H_c$, dd, $J_{(1,2)}$ =13.2Hz: $J_{(2,3)}$ =6.4Hz), 7.17-8.25 (8H, m, Ar - H); ^{13}C NMR (400 MHz, $CDCl_3$): δ 155.57 (C=N), 88.24 (C-O), 45.71 (CH_2), 123.42-133.84 (Ar-C).

Density functional theory (DFT)

The computations were performed using the Gaussian 09W software, which includes the DFT package and uses the B3LYP exchange-correlation method. For the derivatives, we used the 6311G (d, p) basis sets[49]. Gauss View 6 software made it easier to visualize the molecular structures[38].

Molecular docking analysis

Docking is a technique that predicts the orientation and form of ligands in the active site of a target. The goal of docking research is to create precise models of structures in order to gain understanding of how substances behave. Using the Auto dock vina 1.5.7 online tool, the synthesized compounds (ligands) were docked with the 4URO protein. Protein Data Bank provided the 3D crystal structure of the protein (PDB ID:4URO)[32]. ChemDraw 8.0 ultra version software was used to create the ligand's 2D and 3D structures. Discovery Studio 2021 is used to analyzed the final results.

ADMET Analysis

The Swiss ADME web tool was used to calculate the absorption, distribution, metabolism, and excretion properties of synthesised compounds. The Swiss ADME predictor provides details on a compound's total polar surface area, number of hydrogen donors, hydrogen acceptors, and rotatable bonds and pharmacokinetic properties.[48] To find the rate of absorption (%) following equation (17) was used.

$$\% \text{ ABS} = 109 - (0.345 \times \text{TPSA}) \quad \ldots (17)$$

Protoxicity software was used to evaluate the toxicity effects of the newly synthesized compounds.

Antimicrobial activity

Antibacterial assay

The antimicrobial susceptibility test was performed using the Kirby-Bauer disc diffusion method[38]. The antibacterial activity of the synthesized isoxazoline was examined using two Gram-positive and two Gram-negative bacterial strains, including *Staphylococcus aureus*, *Enterococcus faecalis*, *Escherichia coli*, *and Klebsiella pneumonia*. To create Mueller-Hinton Agar (MHA) plates, sterilized Petri dishes were filled with 15 mL of melted medium. For almost five minutes, the plates were left to harden. To guarantee correct inoculation, a sterile cotton swab was used to evenly distribute the bacterial suspension across the MHA plates' surface. The plates were then allowed to dry for five minutes. The wells were filled with 20 µL of each test concentration of synthesized isoxazoline (1–8). For 24 hours, the plates were incubated at 37°C. Antibacterial activity was tested by measuring the diameter of the inhibition zone (in mm) produced around the well, which represents the extent of bacterial growth inhibition.

Antifungal assay

The antifungal susceptibility assay was conducted by means of the Kirby–Bauer disc diffusion method[38]. The antifungal efficacy of the synthesized isoxazolines was evaluated against two fungal strains, namely *Candida albicans and Candida auris*. Each 15-cm Petri dish was given 20 mL of Sabouraud Dextrose Agar, which was then allowed to harden. Wells were drilled into the agar surface with a sterile cork borer. The test sample fractions were evaluated at various concentrations (made in 70% ethanol). 50 µL of each sample (1 mg/mL) was added to the wells. Fluconazole was utilized as the positive control. The plates were incubated at 27°C for 48 hours. Antifungal activity was evaluated by measuring the inhibition zones around the wells, and results were expressed in millimeters (mm). The larger the zone of inhibition, the greater the antifungal activity.

Conclusion

There are eight 3-(4-bromophenyl)-5-substituted phenyl-4,5-dihydro isoxazole derivatives were synthesized from 4-bromophenyl chalcone derivatives by condensation cum cyclization method. The synthesized compounds were characterized by their physical constants, IR, ^{1}H and ^{13}C NMR spectral techniques**.** These stretching frequencies and chemical shifts are correlated with Hammett substituent constant and Swain-Lupton's constants. In single linear regression analysis, some of the Hammett substituent constant produce poor correlations, but in multilinear regression analysis all shows satisfactory correlations. The antimicrobial screening results reveal that compound **8** act as a potent antimicrobial agent against examined pathogens. The density functional theory approach and molecular docking study results show the compound **7** and **8** has more

reactivity, polarizability and binding affinity. The ADMET prediction result confirms that all of the synthesised compounds could be effective drug candidates for further pharmacological research.

Acknowledgement

Authors express their thanks to the Department of Chemistry, Gandhigram Rural University, Dindigul for recording NMR spectra of all compounds.

Supplementary Information

Regression analysis results and NMR spectra of all compounds are given in supplementary information. Supplementary information is available in the website https://nopr.niscpr.res.in/handle/123456789/58776.

References

1 Alam W, Khan H, Saeed Jan M, Rashid U, Abusharha A & Daglia M, *Front Chem*, 11 (2023) 19.
2 Shaik A, Kishor P & Kancharlapalli V. *The 23rd International Electronic Conference on Synthetic Organic Chemistry,* 16 (2020) 12.
3 Reheim M A, Abdou M M, Gaby M S, Al-Omari M H A, Abu-Rayyan A, Al-Assy W, Refat H M, Sarhan A A M & Hafiz I S A, *Mol Divers,* 30 (2025) 612.
4 Adole V A, Jagdale B S, Pawar T B & Sagane A A, *S Afr J Chem,* 73(2020) 35.
5 Jiyani R V & Shah R V, *World J. Pharm Res,* 13 (2024) 889.
6 Alshamari A, Al-Qudah M, Hamadeh F, Al-Momani L & Abu-Orabi S S, *Molecules*, 25 (2020) 4271.
7 Al-Rubaye H I, Mohammed Abbas Z, Jinzeel N A & Askar F W, *J. K. Chem. Sci,* 3 (2024) 319.
8 Kumar G & Shankar R, *Chem Med Chem,* 16 (2021) 447.
9 Aiswarya P, Bhanu Sridhar M & Kavitha L, *Int J Engg Res Technol*, 9 (2020) 386.
10 Buoli M, Grassi S, Ciappolino V, Serati M & Altamura A. C, *Clin Neuropharm,* 40 (2017) 92.
11 Cox J H, Seri S & Cavanna A E, *Adv Ther,* 31 (2014) 288.
12 Bartzatt R, *Anti-inflam Anti-aller Agent Med Chem,* 13 (2014) 17.
13 Majewsky M, Wagner D, Delay M, Bräse S, Yargeau V & Horn H, *Chem Res Toxicol,* 27 (2014) 1828.
14 Kalidhar U & Kaur A, *Res J Pharm Biol Chem Sci*, 2 (2011) 1135.
15 Lainson J C, Daly S M, Triplett K, Johnston S A, Hall P R & Diehnelt C W, *ACS Med Chem Lett*, 8 (2017) 857.
16 Mani S S R & Iyyadurai R, *Int J Immun Pharm,* 30 (2017) 301.
17 Sjöstedt N, Amaeze O U, Van Den Heuvel J J M W, Stage T B, Koenderink J B, Isoherranen N, Kidron H & Järvinen E, *Clin Transl Sci*, 19 (2026) e70487.
18 Faulds D, Goa K L & Benfield P, *Drugs,* 45 (1993) 1040.
19 Zafar S, Armaghan M, Khan K, Hassan N, Sharifi-Rad J, Habtemariam S, Kieliszek M, Butnariu M, Bagiu I C, Bagiu R V & Cho W C, *Biomed Pharm,* 165 (2023) 115039.
20 Geetha C, Rajakumar P R, Christuraj P, Manikandan V, Arulkumaran R & Thirunarayanan G, *J Adv Sci Res*, 10 (2019) 166.
21 Arzine A, Hadni H, Boujdi K, Chebbac K, Barghady N, Rhazi Y, Chalkha M, Nakkabi A, Chkirate K, Mague J T, Kawsar S M A, Al-Houari G, Alanazi M & El-Yazidi M, *Molecules,* 29 (2024) 3366.
22 Swain C G & Lupton E C J, *J Am Chem Soc*, 90 (1968) 4328
23 Sakthinathan S P, Vanangamudi G & Thirunarayanan G, *Spectrochim Acta,* 95A (2012) 700.
24 Sathiyamoorthi K, Mala V, Sakthinathan S P, Kamalakkannan D, Suresh R, Vanangamudi G & Thirunarayanan G, *Spectrochim Acta,* 112A (2013) 256.
25 Suresh R, Kamalakkannan D, Mala V, Sathiyamoorthi K, Sundararajan R, Sakthinathan S P, Arulkumaran R, Vanangamudi G & Thirunarayanan G, *Adv. Appl. Res,* 7 (2015) 27.
26 Shaban M M, El Basiony N M, Radwan A B, El-Katori E E, Abu-Rayyan A, Bahtiti N H & Abdou M M, *ACS Omega,* 8 (2023) 30080.
27 Pallavi H M, Al-Ostoot F H, Vivek H K & Khanum S A, *J Mol Struc,* 1250 (2022) 13.
28 Dinesh Kumar N, Rajmohan S, Selvakumar K, Rajamanickam D, Thirunarayanan G & Swaminathan M, *J Mol Struc*, 1343 (2025) 142824.
29 Bouzammit R, El Hachlafi N, El Fadili M, El Khabchi M, Kanzouai Y, Salghi R, Alanazi M M, Chalkha M, Pop A M, Gal E, Gaina L I & Al Houari G, *Sci Rep*, 15 (2025) 31103.
30 Hissam M A, Ngaini Z, Patrick Mesebasio S I & Jefree Shahren D A, *Discov Appl Sci*, 7 (2025) 654.
31 Jas M J, Marimuthu G & Prithivirajan B, *Indian J Chem*, 63 (2024) 822.
32 Falah Azeez Z, Ali Khaleel L & Ali Kadhim Kyhoiesh H, *Res Chem*, 12 (2024) 20.
33 Abdelazeem N M, Aboulthana W M, Hassan A S, Almehizia A A, Naglah A M & Alkahtani H M, *Saudi Pharm J*, 32 (2024) 14.
34 Van Norman G A, *JACC: Basic Trans Sci*, 4 (2019) 854.
35 Noga M, Michalska A & Jurowski K, *Arch Toxicol*, 97 (2023) 1700.
36 Gayathri P, Mayavel P, Muthuvel I, Balasundari S, Sudha P, Usha V, Ranganathane K, Sathiyendiran V, Krishnakumar B, Rajasri S, Veeravelan K & Thirunarayanan G, *Indian J Chem*, 65 (2026) 822.
37 Weyesa A, Eswaramoorthy R, Melaku Y & Mulugeta E, *Adv Appl Bioinform Chem*, 14 (2021) 144.
38 Bauer A W, Kirby W M M, Sherris J C & Truck M, *Am JClin Pathol*, 45 (1966) 493.
39 Gayathri P, Koteswara Rao Anam, Divya J, Balasundari S, Sudha P, Mayavel P, Muthuvel I, Usha V, Sathiyendiran V, Krishnakumar B, Ranganathan K, Dinesh kumar, N, RajasriS & Thirunarayanan G, *Indian J Chem*, 64 (2025) 1097.
40 Gayathri P, Divya J, Muthuvel I,Usha V, Malar Retna& Thirunarayanan G, *Indian J Chem*, 64 (2025) 670.
41 Gayathri P, Muthuvel I, Mayavel P, Ranganathan K, Usha V, Mala V & Thirunarayanan G, *Ovidius Univ Annal Chem*, 36 (2025) 66.
42 Nalini S, Gayathri P, Divya J, Muthuvel I, Thirumurthy K, Mayavel P, Dinesh K N & Thirunarayanan G, *Russian J Org Chem*, 60 (2024) 2242.
43 Divya J, Gayathri P, Muthuvel I, Suguna S & Thirunarayanan G, *Chem Sel*, 9 (2024) e202402276.

44 Mayavel P, Divya J, Gayathri P, Balasundari S, Usha V, Muthuvel I, Krishnakumar Balu, Shivakumara K N, Gurusamy R, Thirunarayanan G, *Res Chem Intermed*, 50 (2024) 4503.
45 Nalini S, Divya J, Gayathri P, Muthuvel I, Thirunarayanan G, Manikandan V & Usha V, *Indian J Chem*, 63 (2024) 557.
46 Gayathri P, Mayavel P, Muthuvel I, Balasundari S, Sudha P, Divya J, Govindarajan D, KrishnakumarB, Ranganathan K, Usha V, Devika K & Thirunarayanan G, *Indian J Chem*, 65 (2026) 348.
47 Arasu B V, Thirunarayanan G & Kulanthaivel S, *Disc Chem*, 3 (2026) 168.
48 Venkatraman R, Divya J, Gayathri P, Muthuvel I & Thirunarayanan G, *Indian J Chem,* 64 (2025) 475.
49 Sudha P, Balasundari S, Gayathri P, Rajasri S, Muthuvel I, Sivakumar P, Manikandan V, Srinivasan S, Sathiyendiran V & Thirunarayanan G, *Ovidius Univ Annal Chem*, 36(2025) 149.
50 Vijayakumar S, Vanangamudi G & Thirunarayanan G, *World Scientific News* 54 (2018) 152.